The winners of the 2018 CAP Best Student Presentation Competition at the CAP Annual Congress, 2018 June 11-15, in Halifax, NS, are posted on the CAP's website at https://www.cap.ca/congress-conference/past-congress/congress-2018/. The extended abstracts of those winners who submitted them for publication are reproduced below. Ed.

Magnetic Resonance Imaging of Fast Turbulent Gas Flow

by Amy-Rae Gauthier[1] and Benedict Newling

The problem of turbulence has been called "the last unsolved problem of classical physics". While there is no universally accepted definition of turbulence, most physicists have some intuitive sense of the difference between laminar and turbulent flow. Imagine stirring milk into your coffee: notice the coherent structures that form when you first pour in the milk, then see how those structures become incoherent as you stir until you are left with a homogeneous mixture. This is the effect of turbulence.

In any fluid flow system, the velocity field is one of the most important quantities we can measure. To aid in our discussion, it is convenient to introduce the Reynolds decomposition, which separates the velocity field into a time averaged velocity field, $\bar{v}_t$, and a turbulent fluctuation term, $v'(t)$, i.e.,

$$v(t) = \bar{v}_t + v'(t)$$

In a laminar flow, the turbulent fluctuation term would be zero, and so the time-averaged velocity field would be the total velocity field. In this sense, turbulent flow can be characterized as any flow in which the $v'(t)$ term is non-zero [1].

Measuring turbulent flow is a formidable challenge. The difficulty lies in its sensitivity to geometric differences, that is, invasive measurements will alter the velocity field. For this reason, many common flow measurement techniques are not well-suited to turbulent flows. Magnetic Resonance Imaging (MRI) is a versatile and non-invasive technique which can be modified such that measurements are sensitive to turbulent motion. In this article, two fast-flowing turbulent systems will be introduced as examples of the information that can be gleaned from MRI measurements.

Summary

Turbulent gas flow is quantified using motion-encoded SPRITE magnetic resonance imaging to measure the time-averaged velocity field and eddy self diffusivity.

Amy-Rae Gauthier
<Amy-Rae.P.Gauthier@unb.ca>

and

Benedict Newling
<bnewling@unb.ca>

UNB MRI Centre, Department of Physics, University of New Brunswick, 8 Bailey Drive, Fredericton, NB, E3B 5A3

MRI and the Motion-Encoded SPRITE Sequence[1]

MRI is non-invasive, inherently three dimensional, and can measure flows that would otherwise be invisible to optical techniques. The trade-off is that the fluid must be magnetically susceptible, which is why sulfur hexafluoride gas is used in these experiments rather than air. In SF_6, the fluorine nuclei have spin magnetic moments which align with the magnetic field. The sample space is divided into voxels, and each voxel contains on the order of 10^{41} nuclei. The spin magnetic moments are summed to create a bulk magnetization vector which precesses about the magnetic field at a frequency given by Larmor's equation:

$$\omega = \gamma B$$

where ω is the frequency of precession, γ is the gyromagnetic ratio which is unique to each magnetically susceptible nucleus, and B is the magnetic field. The versatility of MRI lies in the manipulation of B; i.e., different combinations of spatial magnetic field gradients can be applied to sensitize ω to various physical phenomena, including motion.

The particular combination of sample excitations and magnetic field gradients, collectively known as a pulse sequence, used in these measurements is the motion-encoded SPRITE sequence (Single Point Ramped Imaging with T_1 Enhancement) [2]. A plot of the magnetic field gradients applied over time for a single data point acquisition is pictured in Fig. 1. To achieve motion-sensitization, two

1. Amy-Rae Gauthier received 1st place in the CAP Best Student Oral Presentation competition at the 2018 CAP Congress at Dalhousie U.

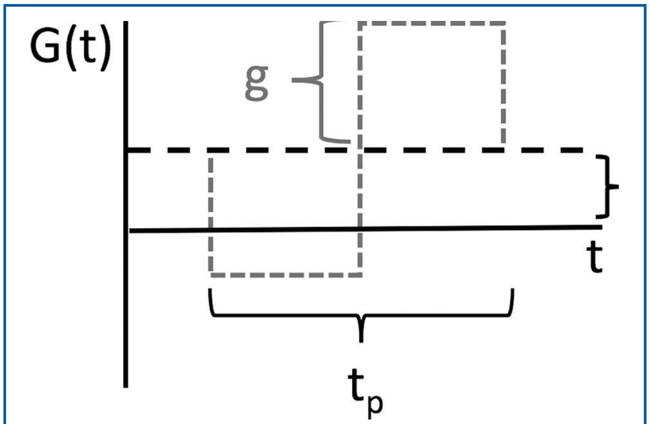

Fig. 1 The spatial magnetic field gradient applied for one data point acquisition in the motion-encoded SPRITE pulse sequence. Two gradients are superimposed: the imaging gradient with magnitude G, and the motion-encoding gradient with magnitude g. The time between excitation and detection of the signal is t_p.

magnetic field gradients are superimposed. The constant gradient is known as the imaging gradient, and the bipolar gradient is known as the motion-encoding gradient. The time t_p represents the time between excitation of the sample via a radio-frequency pulse, and detection of the resulting signal.

The motion-encoded SPRITE sequence introduces a Larmor frequency in the sample space that is dependent on both position and velocity. Integrating the Larmor frequencies over the time t_p results in an expression for the phase accumulation of the magnetization vector:

$$\phi = r\left(\gamma t_p G\right) + \overline{v}_t \left(\frac{\gamma t_p^2}{4} g\right) + \ldots$$

The first term contains information on the position and depends only on the imaging gradient G. The second term contains the time-averaged velocity field $\overline{v}_t$ and depends only on the motion-encoding gradient g. This expression is a Taylor series expansion of the position, so higher order terms would depend on acceleration, jerk, etc. and these terms are assumed to be negligible. This expression is also the equation of a line for a plot of phase $ø$ vs. g, and the slope of this line is proportional to $\overline{v}_t$. In this way, motion-encoded SPRITE can be used to directly measure the time-averaged velocity field of a turbulent flow, i.e., the first term in the Reynolds decomposition.

The signal amplitude also contains information relevant to turbulence. Signal amplitude is proportional to the length of the bulk magnetization vector, so if there is a wide distribution of accumulated phase in a voxel, the signal is attenuated. In laminar flow, all particles of gas from a particular voxel take approximately the same trajectory through the magnetic field gradients,

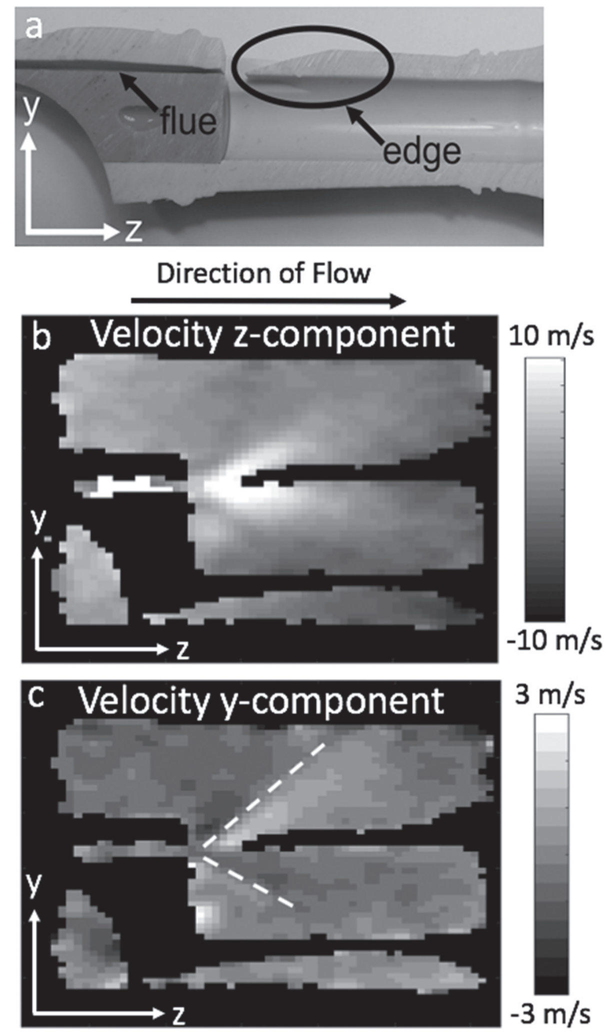

Fig. 2 (a) The cross-section of a recorder nominally identical to the recorder used in the measurements. The important geometric features are the flue and the edge. (b) The central slice of the *z*-component of the time-averaged velocity. (c) The central slice of the *y*-component of the time-averaged velocity.

so the phase distribution is narrow. In turbulent flow, gas particles take different trajectories through the magnetic field gradients, so the voxel contains a much wider phase distribution and the signal is attenuated. The attenuated signal is modelled using a tensor quantity we call the *eddy self diffusivity*, as follows

$$\boldsymbol{D} \cdot \boldsymbol{b} = -\ln\left(\frac{S_o}{S}\right)$$

$\frac{S_o}{S}$ represents the ratio between signal attenuated due to the presence of motion-encoding gradients and signal acquired with

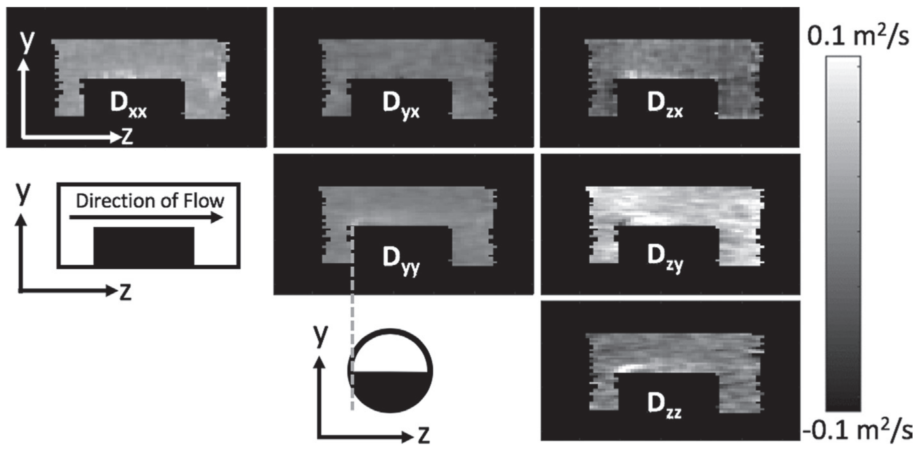

Fig. 3 The central slice of the eddy self diffusivity tensor with sketches of the pipe geometry.

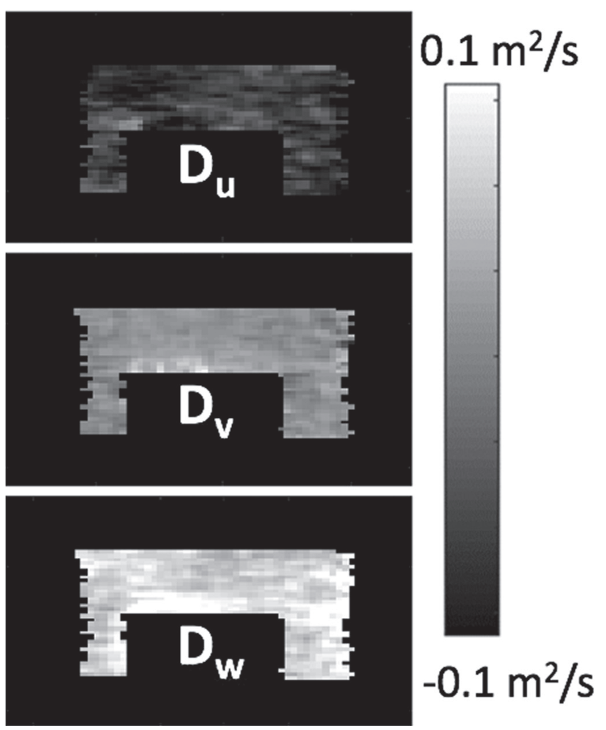

Fig. 4 The three eigenvalues of the eddy self diffusivity tensor in Fig. 3.

only imaging gradients. ***D*** is the eddy self diffusivity tensor, which contains six independent components. ***b*** is called the "b-factor" and is a tensor quantity which describes how sensitive the measurement is to diffusivity. Taking measurements with six different b-factors creates a system of six equations and six unknowns, so all components of the eddy self diffusivity tensor can be calculated. The greater the value of the eddy self diffusivity, the greater effect the turbulent fluctuation term, $v'(t)$, has in that region of the sample space [3]. This is how motion-encoded SPRITE can provide information about the turbulent fluctuation term in the Reynolds decomposition.

EXAMPLES OF TURBULENT FLOW

To demonstrate the effectiveness of the time-averaged velocity field measurements, we use the example of gas flow through a recorder. The recorder has two main geometric features: the flue, which is a narrow channel in the mouthpiece that generates a jet, and the edge, which is a sharp obstruction that generates the oscillations needed to produce sound (see Fig. 2a). According to simulation studies of the recorder (e.g., [4]) the fastest speeds should appear in the flue and the gas should oscillate above and below the edge.

The time-averaged velocity field measurements are consistent with these expectations. The *z*-component of the velocity, pictured in Fig. 2b, shows that the speed is greatest in the flue at 20 m/s. Adjacent to the edge, the speed is reduced to around 10 m/s, and the bulk of the fluid is moving in the positive *z*-direction. The *y*-component of velocity, pictured in Fig. 2c, shows that the speed is positive immediately above the edge, and negative immediately below the edge in the space contained by the dashed white lines. This suggests that the gas is oscillating above and below the edge as expected. Furthermore, the maps suggest that recirculation is present, as evidenced by the change in sign of the speed outside the space enclosed by the dashed white lines. These results are broadly consistent with simulations and theoretical models of the recorder, and details regarding these results can be found in [5].

To demonstrate the measurement of the eddy self diffusivity, we use a much simpler geometry: a cylindrical pipe with a hemi-cylindrical obstruction, drawn in Fig. 3. Gas is moved through the pipe at speeds on the order of 10 m/s. Intuitively, we expect the region where the gas encounters the edge of the obstruction to be where the turbulent fluctuations have the greatest effect. For the central cross-section of the pipe, all six components of the eddy self diffusivity tensor are mapped in Fig. 3. The *ZZ* and *ZY* components of the tensor show a bright spot adjacent to the edge of the obstruction, so these results are consistent with our expectations.

The eddy self diffusivity tensor can be manipulated further to answer a bigger question: is turbulence in this system isotropic? Typically, in computational fluid dynamics simulations, the turbulence is assumed isotropic to simplify the already complex calculations required. Also, turbulence is often thought of as a completely random phenomenon, so the assumption of isotropy is natural. If turbulence were isotropic in this system, the eddy self diffusivity tensor would have no off-diagonal elements, and all the diagonal elements would be the same. However, the tensor in Fig. 3 has as its principal axes the x, y, and z axes of the MRI system. To test isotropy, the eddy self diffusivity tensor is diagonalized, and if the eigenvalues come out the same, then turbulence is isotropic. Figure 4 shows maps of the three eigenvalues for each voxel in the sample space. They are not the same, and therefore turbulence in this system is anisotropic. Further investigations of this system are currently underway to see if the turbulent anisotropy can be further quantified.

CONCLUSION

The two turbulent systems explored here are examples of how MRI is well-suited to the problem of turbulence because it is non-invasive and naturally three dimensional. In particular, the motion-encoded SPRITE pulse sequence continues to be a robust tool for the measurement of gas flow. The phase accumulation offers a direct measurement of the time-averaged velocity field, which is the first term in the Reynolds decomposition. The signal amplitude contains information about the turbulent fluctuation term, and by modelling the turbulence as an eddy self diffusivity tensor, the turbulent anisotropy can be measured. These two quantities are helpful in quantifying and characterizing turbulence, which can help inform computational and theoretical work in the field.

REFERENCES

1. P.A. Davidson, *Turbulence: An Introduction for Scientists and Engineers*. Oxford University Press, 2009.
2. B. Newling, *et al.* “Velocity imaging of highly turbulent gas flow”, *Phys. Rev. Lett.* **93**, 154503-1-154501-4 (2004).
3. D.O. Kuethe, “Measuring distributions of diffusivity in turbulent fluids with magnetic-resonance imaging”, *Phys. Rev. A* **40**, 4542-4551 (1989).
4. N. Giordano, “Simulation studies of a recorder in three dimensions”. *J. Acoust. Soc. Am.* **135**, 906-916 (2014).
5. A-R Gauthier and B. Newling, “Gas Flow Mapping in a Recorder: An Application of SPRITE MR” Appl. Magn. Reson. DOI: 10.1007/s00723-018-1034-x, in press.